Middle East Technical University

ASE 435 | TERM PROJECT

Development of a Ramjet Engine Design Code and CFD Analysis of Engine Intake for the Design Point Mach Number

Submission date:

05/02/2022

Submitted by:

Kübra Çınar: 2328177

Yusuf Kerim Say: 2245959

Süleyman Aylar: 2317980

Melih Çimen: 2083848

Instructor: Dr. Sıtkı Uslu

Table of Contents

Nomenclature

M	Mach Number
δ	Ramp Angle
θ	Deflection Angle
γ	Specific Heats Ratio
A^*	Throat Area of Nozzle
TSFC	Thrust Specific Fuel Consumption, TSFC = $\frac{\dot{m}f}{T}$
δ_1	First Ramp Angle at the Inlet
δ_2	Second Ramp Angle at the Inlet
δ_3	Third Ramp Angle at the Inlet
ϑ_1	First Deflection Angle at the Inlet
ϑ_2	Second Deflection Angle at the Inlet
ϑ_3	Third Deflection Angle at the Inlet
M_0	Free Stream Mach Number
M_1	Mach Number Downstream of the First Shock
M_2	Mach Number Downstream of the Second Shock
M_3	Mach Number Downstream of the Normal Shock
M_4	Mach Number at the Inlet of the Fan
PR_1	Total Pressure Ratio Across the First Shock at the Inlet
PR_2	Total Pressure Ratio Across the Second Shock at the Inlet
PR_3	Total Pressure Ratio Across the Third Shock at the Inlet
PR_n	Total Pressure Ratio Across the Normal Shock at the Inlet
PRF	Total Pressure Recovery Factor of the Inlet
η_{th}	Thermal Efficiency, $\eta_{th} = \frac{(1+f)U_e^2/2 - U_9^2/2}{fQ_R}$
η_p	Propulsive Efficiency, $\eta_\rho = \frac{2x\left(F_n/\dot{m}_0\right)xV_0}{(1+f)x(V_9)^2 - V_9^2}$

θ Primary Nozzle Half Angle

α Secondary Nozzle Half Angle

L_P Primary Nozzle Length

L_s Secondary Nozzle Length

I_{sp} Specific Impulse, $I_{sp} = \frac{F}{g\dot{m}f}$

F_s Specific Thrust, $F_s = \frac{F}{\dot{m}} = (1 + f)V_e - V_0$

1. Introduction

A ramjet uses forward motion of the engine without a compressor in order to compress incoming air. The reason of this is that at zero airspeed, thrust cannot be produced by ramjets, and ramjets cannot provide forward motion to aircraft from standstill. Thus, until thrust is produced, aircraft which is powered by a ramjet needs assisted take-off. To get the most efficient performance by ramjet, it must operate at conditions which are supersonic speeds around Mach 3, and it can continue to its operation up to 6 Mach.

The project's goal is improving a one-dimensional (1D) design tool (code) that uses analytical and/or empirical, semi-empirical correlations to forecast the performance of a ramjet engine at various flight speeds, with Mach values ranging from 2 to 6. In this project one of the most important aspects is number of ramps which are used for the intake design. When the flight speed is increased, number of ramps are raised. In addition, realizing condition of intake compression is another important point whether an external, internal, or mixed compression is chosen for the design.

2. Theory & Methodology

2.1. What is Ramjet?

A ramjet is an air breathing propulsive engine and compress air without having any compressor, turbine or moving parts. Air is forced to rise its pressure and temperature by using its velocity at the inlet of ramjet. Air is highly slowed down and passes through the inlet and moves to the combustion chamber. Combustion starts at subsonic speeds and with the combustion, air expands and reaches supersonic speeds.

The important limitation of ramjet is they cannot start from zero speed. Because they need to be moving in order to force gas into the intake. Therefore, around Mach 3 is a good starting point for a ramjet engine. It operates between Mach 3 and 6. If we want to try to push a ramjet up to higher speeds, ram-effect of forcing the air into the engine, raises the pressure and temperature up to levels so that the temperature become too high to be able to achieve efficient combustion.

Ramjet engines have a very simple geometry. They have only three main stationary parts which are a diffuser region at the entrance, a combustion chamber in the middle and a nozzle at the exit. The duty of the diffuser is to increase pressure and temperature of the air.

Ramjet engines will work only supersonic conditions. Since the flow is supersonic, scientists tweaked the shock wave concept to increase the diffuser pressure. In a shock wave the high pressure and temperature is there only in a narrow region. However, when many such shock waves come together inside a cylinder without diffuser, a thick volume of high pressure and temperature air is formed inside the cylinder. It forms automatic compression action with the help of shock waves and called as ram-effect. This high pressure and temperature air can create effective combustion in the combustion chamber. Hydrogen and kerosene are commonly used as fuel for ramjet engines. The combustion chamber further increases the gas temperature and also fluid velocity. According to Newton's third law, the greater the exhaust jet speed, the more thrust rocket derives. To increase the speed of jet further, a converging diverging nozzle is also added at the exit. Even though this simple diffuser arrangement achieves very high-pressure boost, if the combustion pressure exceeds limits the shock front will be blown out resulting in compressed air spilling out around the front of the cylinder. This spill limits the speed of ramjet to 1.2 Mach. For the further improvements of ram-effect, aerodynamically designed inner body

added. With this body called diffuser, area allocated for the air is actually decreasing along with the flow. For supersonic flow, when the area decreases the pressure increases so that in ramjet the majority of the pressure rise happens due to the shock effect of oblique shock wave. When air hits the nose of inner body it deflects with some angle forming an oblique shock wave. This oblique shock wave hits the outer tube and deflects multiple times and is finally terminated by a normal shock wave. In this case, the air spill out does not happen and high Mach number for the ramjet engines were able to achieve.

The airflow speed through the ramjet is so high that the mixing of fuel completes within 2 to 5 milliseconds. For complete mixing of fuel and air, flame holder is used which helps to maintain continuous combustion similar to conventional gas turbine engines. It also stops the flame from blowing out by sheltering it. Subsonic speeds support efficient combustion.

Ramjets are the most efficient in the speed range of Mach 3 to 6. When travelling at low speed, the thrust isn't sufficient to overcome the drag. As a result, the stand-alone ramjet engine is not feasible. It needs initial speed or solid booster to proper engine towards supersonic speeds.

2.2. Applications of Ramjet

Bomarc Missile

World's first long-range anti-aircraft missiles are the supersonic Bomarc missiles, and these missiles produced by Boeing. These missiles consist of Marquardt ramjet engines, connected to the underside of the missile by pylons, propelled it at Mach 2.5 to a range of quarter thousands of miles.[1]

Figure 1: Bomarc Missile [1]

Lockheed D-21 Drone

Operation of the Lockheed D-21 unmanned drone was start at Mach 3 A12 Blackbird's top rear fuselage from pylon mounting. Lockheed D-21 Drone is powered by Marquardt RJ43-MA-20 Ramjet. [2]

Figure 2: Lockheed D-21 Drone [2]

2.3. Inlet Types

Ramjet engines consist of intakes, combustors, and nozzle. Since there is no need to compressors and as a result no need turbines, the entire compression process is accomplished in the intake of a ramjet. The air that comes through the inlet is supersonic and it can't be directly used for the combustion. Because complete combustion can't be achieved with the mixture at such speeds. The diffuser slows the incoming flow of air which increases pressure and temperature before combustion occurs and decelerated flow helps to achieve appropriate combustion.

The ideal ram pressure ratio across the intake which related with Mach number is:

$$\frac{P_{O_a}}{P_a} = \left(1 + \frac{\gamma-1}{2} M^2\right)^{\frac{\gamma}{\gamma-1}} \quad (1)$$

However, it is not possible to produce isentropic compression in supersonic range due to the shock waves. Shock gives a sudden discontinuity in airflow and changes pressure abruptly. Having pressure increase look advantageous but full isentropic compression can't be achieved with turbulence. The stronger the shock wave produced, the greater the losses. Therefore, instead of a strong shock wave having multiple weak ones could increase the intake efficiency and taken into account while designing it. Three different types of supersonic intakes are used, depending on the location of the shock waves produced in the intake which are internal compression, external compression, and mixed-flow compression.

2.3.1. External Supersonic Compression Intakes

To create oblique shocks ramps are used by external compression intakes and this cause to increase on static pressure and temperature and decrease on the velocity of the flow.

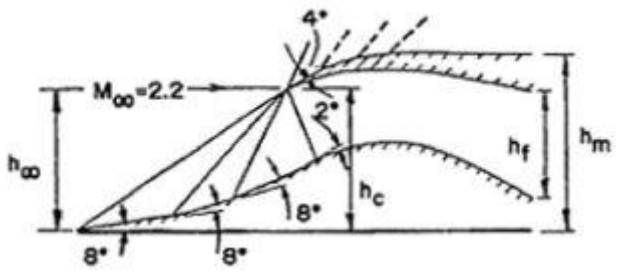

Figure 3: External Compression with 3 Oblique Shocks [3]

In Figure 3, three oblique shocks are examined with external compression intake on the cowl lip. To have subsonic flow, first oblique shock is observed, and it is followed by normal shocks which are much more dissipative than oblique shocks. To decrease the velocity of the flow progressively, oblique shocks are used and with normal shocks flow is made subsonic. This progress increases the efficiency of intake in the scope of total pressure recovery.

Austrian physicist Klaus Oswatitsch proved that to achieve maximum pressure recovery for a two-dimensional compression system of n-1 oblique shocks and one normal shock, for all shocks in the system, the Mach number perpendicular to the shock should be same.

$$M_1 sin\beta_1 = M_2 sin\beta_2 \ldots = M_{n-1} sin\beta_{n-1} \quad (2)$$

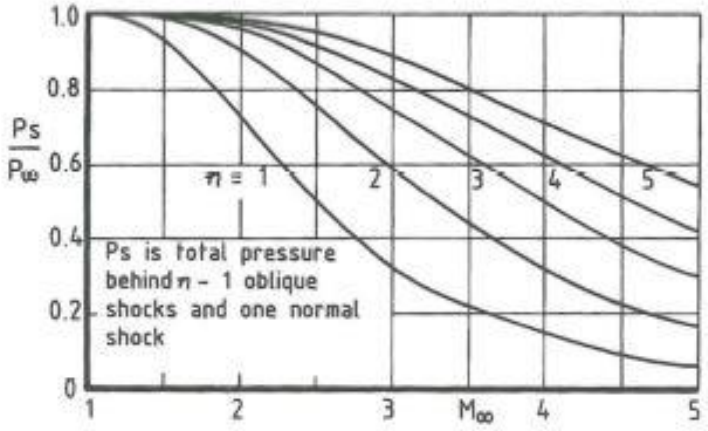

Figure 4: Pressure Recovery vs Number of Oblique Shocks [3]

Figure 4 shows that to have more pressure recovery factor, number of oblique shocks should be increased. Also, by the help of equation 1, curves can be calculated.

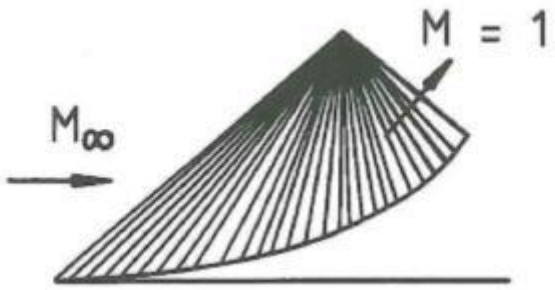

Figure 5: Isentropic Compression [3]

Creating infinitely many oblique shocks provide isentropic compression and increase total pressure recovery. As it can be seen from Figure 5, by the help of curved intake, this can be done.

Isentropic compression is the best option to get maximum total pressure recovery. On the other hand, when drag and production costs are taken into account, this method puts question marks in minds. The reason of this, it must divert the flow away from the intake's main axis to a greater amount than less efficient compression systems. Pressure losses are observed when the flow

turned back in the subsonic diffuser again. In addition, the cowl lip must be oriented so that it matches the flow's turning angle. This will result as an increase on wave drag of the cowl lip.

In conclusion, high turning angels are the main problem of the external intakes. They cause to have more wave drag and less internal pressure. Therefore, they need to be operated less than Mach 2. [3]

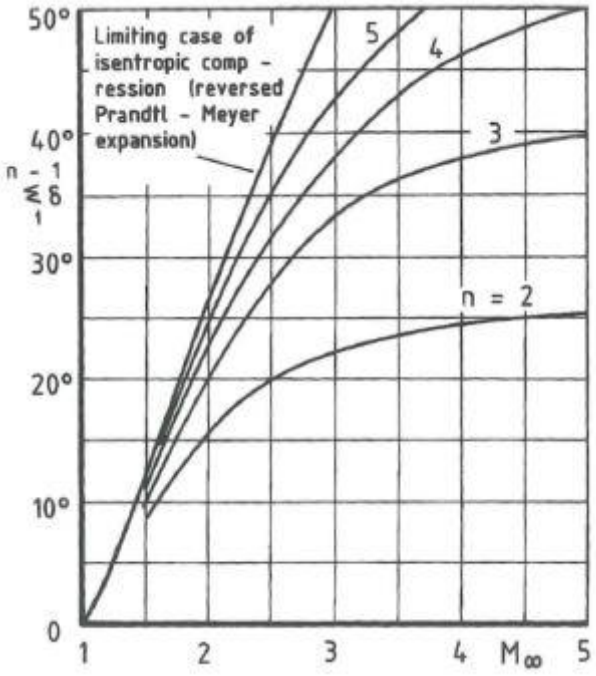

Figure 6: Turning Angles for Optimum External Compression [3]

2.3.2. Mixed Supersonic Compression Intakes

A mixed supersonic compression intake as it can be understood by its name, it is the combination of internal compression and external compression [3]. Externally generated oblique shocks reflected internal oblique shocks, and a normal shock wave are used by mixed compression intake at the throat region to provide compression. It tries to get positive effects of external compression intake which are low boundary layer effects, and internal compression intake's low drag and higher-pressure recovery. On the other hand, there is still negative effects of internal compression intake on mixed compression intakes. There are still effects of boundary layer. Moreover, external intake shorter and lighter than mixed compression intake. Against all ods, at above Mach 2, mixed compression intakes are preferred since too much drag is produced by external intake because of its turning angle.

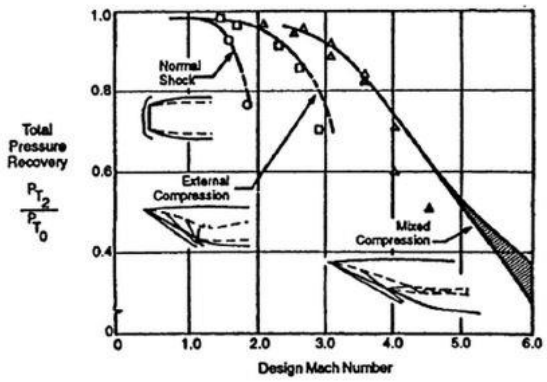

Figure 7: Pressure Recovery for External and Mixed Intakes [3]

To give proper control of the shock wave placement, it also requires variable geometries in the form of adjustable center bodies, bleeding, and by-pass doors. All of the discussed intake geometries can be further categorized based on their form, which can be two-dimensional or axisymmetric. This corresponds to whether the intake geometry is axisymmetric (rotated around an axis) or two-dimensional (projected along an orthogonal axis), as it can be seen from Figure 8.

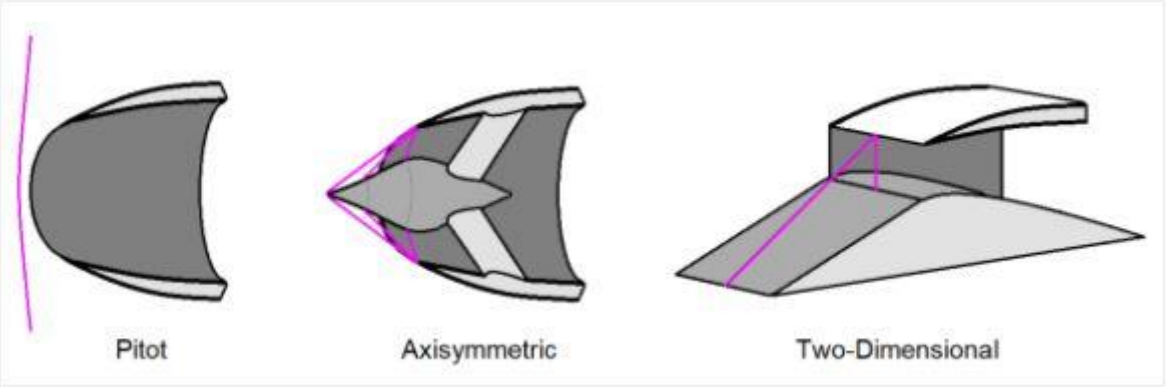

Figure 8: Intake Geometries [4]

2.3.3. Internal Supersonic Compression Intakes

This intake design presents compression through production of a series of internal oblique shock waves, with a normal shock wave located at the throat. It has same principle with external

intake and requires reverse converging-diverging nozzle shape in order to position the shock waves and prevent air spilling.

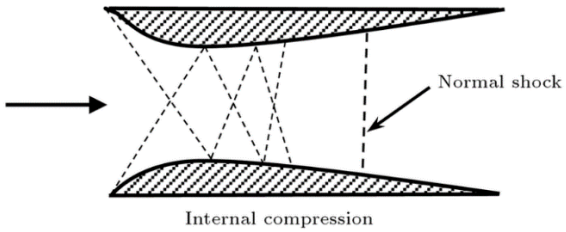

Figure 9: Internal compression intake shock waves

As the flow behind an oblique shock change, it's direction away from the center of intake, it hits the upper surface. Flow has to change direction again, creating a reverse shock. That means flow is always turned back to the axial direction, eliminating flow turning and significantly reducing the drag produced by the cowl lip.

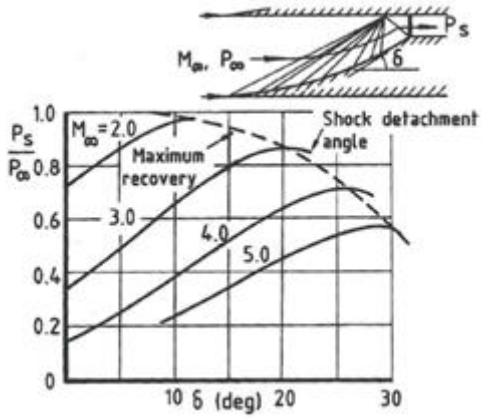

Figure 10: Pressure recovery vs number of oblique shocks for external intake

Internal compression intakes have a high surface area that the incoming flow has to pass over so that significant boundary layer may develop. In addition, if the shock is strong enough, it can separate boundary layer. Due to its shape, internal compression inlet generates a high amount of drag and it is not very easy to integrate the inlet with the whole vehicle. Moreover, the design of internal compression inlet is rather complicated because of complex flow field structure and the need for variable geometry to establish stable flow.[10]

Calculation of the oblique shock angle is done as follows

$$\tan\theta = 2\cot\beta \frac{M_1^2 \sin^2\beta - 1}{M_1^2(\gamma + \cos^2 B) + 1} \tag{3}$$

Then, normal upstream Mach number should be found to find the downstream Mach number. Equation of upstream Mach number as follows

$$M_{n_1} = M_1 \sin\beta_1 \tag{4}$$

Later, by the help of following equation, value of the normal downstream Mach number is calculated.

$$M_{n_2} = \sqrt{\frac{1 + M_{n_1}^2 \frac{(\gamma-1)}{2}}{\gamma M_{n_1}^2 - \frac{(\gamma-1)}{2}}} \tag{5}$$

Finally, calculation of downstream Mach number is done as follows

$$M_2 = \frac{M_{n_2}}{(\sin\beta_1 - \theta_1)} \tag{6}$$

To obtain total pressure ratio, equation which is below should be used.

$$\frac{P_{t2}}{P_{t1}} = \left(\frac{(\gamma+1)M_1^2 sin^2\beta_1}{(\gamma-1)M_1^2 sin^2\beta_1 + 2}\right)^{\frac{\gamma}{\gamma-1}} \left(\frac{(\gamma+1)}{2\gamma M_1^2 sin^2\beta_1 - (\gamma-1)}\right)^{\frac{1}{\gamma-1}} \tag{7}$$

Total pressure recovery factor (PRF) is calculated as follows

$$\text{PRF} = \frac{P_{t5}}{P_{t1}} = \frac{P_{t5}}{P_{t4}}\frac{P_{t4}}{P_{t3}}\frac{P_{t3}}{P_{t2}}\frac{P_{t2}}{P_{t1}} \quad (8)$$

2.4. Combustion Chamber

An internal combustion engine's combustion chamber is where the fuel is burned at a consistent temperature with the help of air and a gas turbine, where mechanical energy is converted from gas pressure.[5]

There are 3 types of combustion chambers:

Multiple Combustion Chamber

In centrifugal compressor engines and the earlier types of axial flow compressor engines, multiple combustion chambers are used. This type of combustion chamber is developed from the early type of Whittle combustion chamber. [5]

The Whittle chamber featured a reverse flow, which was the main distinction. Joseph Lucas Limited developed the straight-through multiple chambers to solve the problem which is pressure loss.

Tubo-Annular Combustion Chamber

The evolutionary gap between multiple and annular types are bridged by the tubo-annular combustion chamber.

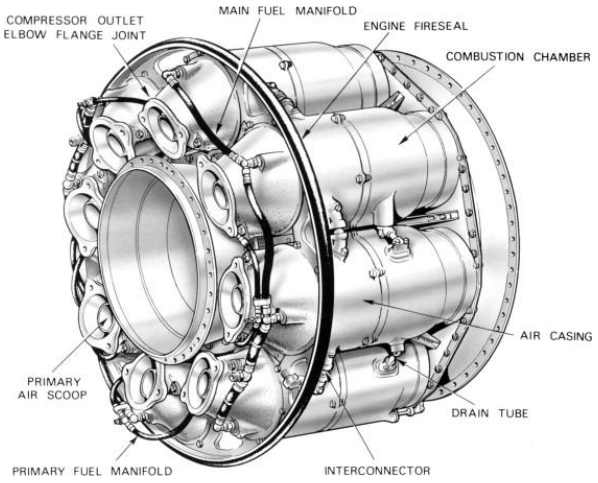

Figure 11: Tubo-Annular Combustion Chamber [6]

Annular Combustion Chamber

One of the parts of annular combustion chamber is single flame tube, it is covered in two casings, one on the inside and one on the outside because of being annular form. Main pros of this chamber are weight reduction. When the length of annular combustion chamber and tubo annular combustion chamber are compared, length of annular combustion chamber is 3/4 of tubo annular chamber with same diameter. This leads to have less weight in annular form than tubo annular combustion chamber.

2.4.1. Selection of Fuel Type

Kerosene mixtures are used in ramjet engines. Kerosene has several properties that make it more suitable for such applications, including a high energy content per unit volume and low vapor pressure, both of which increase friction and altitude performance. Standard commercial aviation jet fuels are designated by the letters Jet A, Jet A-1, and Jet B in the United States. Except for the lower temperature, the Jet A-1 is almost identical to the Jet A. JP 8 and JP4 are largely comparable to Jet A-1 and Jet B. Avtur and Avtag are international names for Jet A-1 and Jet B fuel blends. Similarly, military jet fuel JP5 is also known as Avcat, while JP7 and JP10 fuels are special kerosene blends for high-performance aircraft and missiles. Because kerosene is a mixture of different petroleum products, the chemical formulas listed are approximate and primarily based on the hydrogen to carbon ratio and the molecular weight of the mixtures.

Table 1.1 Properties of Some Aerospace Propulsion Fuels

Fuel	Q_t (MJ/kg)	ρ (kg/m^3)	$Q_{t,v}$ (MJ/L)	ρ_v (kg/L)	W (g/mol)	Chemical Formula[a]	f.p.[b] (°C)	b.p.[c] (°C)
Avgas	44.2	720	31.8	0.72	103	$C_{7.5}H_{15.3}$	−65	46–170
Jet A	43.4	820	34.7	0.82	175	$C_{12.5}H_{24.2}$	−40	150–300
Jet A-1 (JP8)	43.4	800	34.7	0.8	175	$C_{12.5}H_{24.2}$	−48	150–130
Jet B (JP 4)	43.6	760	33.1	0.76	141	$C_{10}H_{20.3}$	−62	73–280
JP 5	43.2	820	35.4	0.82	181	$C_{13}H_{24.8}$	−46	170–300
JP 7	43.5	800	34.8	0.8	136	$C_{12.1}H_{24.4}$	−30	182–288
JP10	42.1	940	39.6	0.94	136	$C_{10}H_{16}$	−79	187
RP-1	43.0	820	35.3	0.82	168	$C_{12}H_{24}$	−48	190–270
Methane	50.0	424[d]	21.2	0.424	16.04	CH_4	−182	−162
Propane	45.5	505[d]	23.0	0.505	44.1	C_3H_8	−188	−42
Butane	44.4	580[d]	25.8	0.58	58.1	C_4H_{10}	−132	−0.3
Ethanol	27.23	794	21.6	0.794	46.07	C_2H_5OH	−115	78.5
Ammonia	18.55	615[d]	11.4	0.615	17.03	NH_3	−77.7	−33.4
Hydrazine	16.68	1013	16.9	1.013	32.05	N_2H_4	1.4	114
Hydrogen	120.2	70[e]	8.42	0.07	2.016	H_2	−259	−253

[a] *Chemical formulas for the Avgas, JP, and RP hydrocarbon mixtures are approximations.*
[b] *Freezing point.*
[c] *Boiling point at 1 atm pressure.*
[d] *Evaluated under the vapor pressure at 15°C.*
[e] *Evaluated at the b.p. and 1 atm pressure.*

Figure 12: Properties of Some Aerospace Propulsion Fuels

Figure 12 shows that all these kerosene mixtures have similar net energy content (O_f), with the main differences being physical properties such as freezing point. Jet B has a lower freezing point than Jet A-1, making it ideal for travel in the stratosphere, where temperatures are around -57°C. However, Jet B has a flash point lower than Jet A-1: -10°C, the temperature at which flash combustion can occur when an ignition source is applied. As a result, Jet A-1 has replaced Jet B as the fuel of choice because it is considerably safer to use. All other fuels in the table 10 can be used in jet engines. However, kerosene blends have the best properties for aviation.[12]

2.4.2. Fuel Injection Systems

A system for injecting fuel into a combustor is known as fuel injection. Fuel is delivered in a series of pulses into the airstream through the combustor of a ramjet engine to assist fuel and air mixing. To build an effective fuel injector, several critical problems must be considered. Total pressure losses caused by the injector and injection operations are particularly important and must be reduced because they affect the engine's thrust. Also mixing and burning process of fuel and air must be provided by fuel injection system.[7]

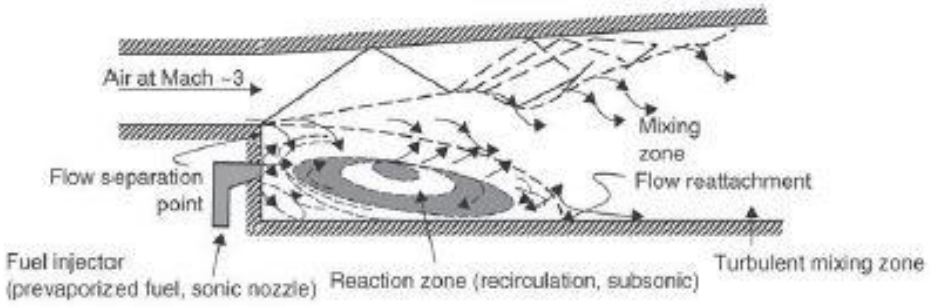

Figure 13: Example of Fuel Injection [8]

Fuel Injection System Types

Normal Fuel Injection

A ramjet's normal fuel injection consists of an injection port on the wall. The fuel is injected into the ramjet at an angle to the air flow. This sort of injection method provides separation zones upstream and downstream of the injector by creating a detached normal shock upstream of the injector.

Transverse Fuel Injection

Parallel and conventional fuel injection are combined in transverse fuel injection. The fuel is injected at an angle between normal and parallel to the flow in a transverse injector. Transverse injection eliminates some of the drawbacks of conventional injection, but it necessitates a higher injection pressure to attain the same penetration height into the air flow. The overall pressure loss of the ramjet increases as the injection pressure rises, lowering the engine's efficiency.

Ramp Injectors

Parallel injection results are used by the ramp injector. Ramps with fuel injectors on the trailing edge of the ramp pumping fuel parallel to the flow were introduced to provide axial velocity to the flow near fuel injection. Counter-rotating vortices were formed by the flow over the ramps, which boosted mixing. The ramps create shocks and expansion fans as a result of the ramjet's supersonic flow, which causes pressure gradients that increase mixing. The following two types of ramps were used in Figure 13:

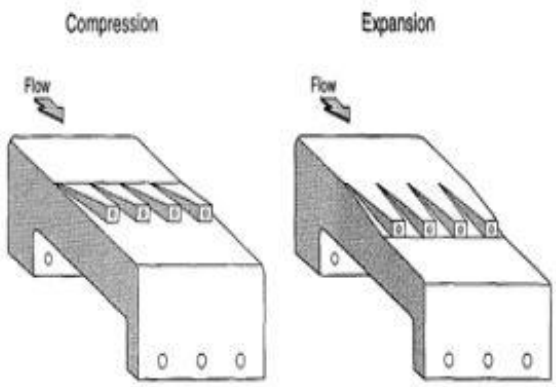

Figure 14: Ramps Used for Mixing [7]

Expansion ramps generate troughs in the floor, while compression ramps are elevated above it. Shocks form at the bottom of the ramp in compression ramps and in the recompression zone at the bottom of the trough in expansion ramps. The combustion efficiency and mixing for the two ramp designs changed due to the different shock sites. Compressor ramps provided a greater vortex and increased fuel/air mixing, whereas expansion ramps had higher combustion efficiency.

Strut Injector

Strut mixing devices are equipped in a variety of shapes and sizes, with both normal and parallel injection methods available. A vertical strut with a wedge leading edge makes up the majority of the struts. The strut is connected to both the top and bottom combustion parts of the combustion chamber. The fundamental benefit of this technique is that it permits fuel to be injected into the heart of the airflow while maintaining consistent radial spread. In addition, the shock caused by the strut's leading edge improves the mixing of air and fuel.

Baronage Injection System

Figure 15 illustrates the baronage injection unit's basic configuration. The kerosene is pumped into a mixing zone through a central tube, and the hydrogen is injected into the annular space around the kerosene tube. Gas bubbles into the liquid in the mixing zone. The two-phase flow is then injected through the injection hole into the ramjet combustor.

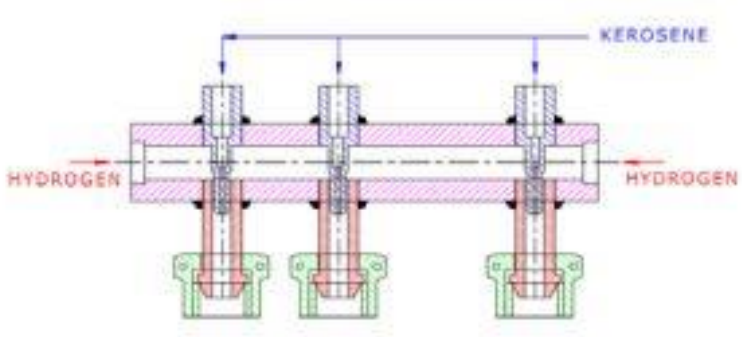

Figure 15: Baronage System [7]

Pulsed Injector

Fuel is injected in a continuous stream from injection ports into the combustion chamber, where it ignites. This method of injection injects the gasoline in a series of pulses, allowing the fuel and air to mix more thoroughly. Combustion takes place more quickly and efficiently, resulting in a higher thrust output. The interval between pulses is determined by free stream conditions and is timed to ensure near-stoichiometric combustion. The fact that combustion is always in a transitory state and never reaches a steady state condition is an advantage of this technology.

Fuel is injected as a series of pulses into the airstream flowing through the ramjet engine's combustor to encourage fuel and air mixing.

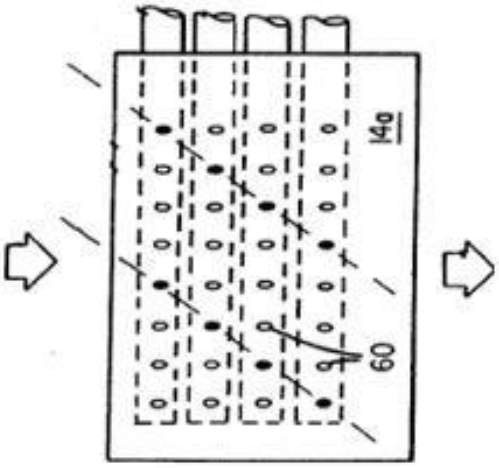

Figure 16: Pulsed Fuel Injection [7]

2.5. Nozzle

The purpose of Nozzle is to increase the magnitude of thrust. As a result, the nozzle design has a significant impact on thrust. To gain higher thrust, the kinetic energy must be high, and the velocity of the exhaust gas must be raised to get more kinetic energy. Apart from kinetic energy, the nozzle pressure ratio and the expansion process are also key factors in achieving high thrust. As a result, the most effective way to generate the highest thrust is to use a properly inflated nozzle with equal exit (P_e) and ambient (P_a) pressures. The first stage in nozzle design is to determine the geometry. Convergent nozzles should be employed for subsonic speed, higher thrust, and smaller weight. To generate more thrust and smaller weight at supersonic speeds, a convergent divergent nozzle should be used.

Flow Through a Convergent Divergent Nozzle

When compared to a reference reservoir pressure, the ambient pressure for C-D nozzles gradually decreases. In the meantime, the flow in the convergent segment accelerates until it reaches sonic velocity near the throat (minimum area section). The flow velocity does not increase as the ambient pressure is reduced more. However, as the flow passes through the throat and into the divergent portion, it accelerates even more to supersonic speeds, as shown

in Figure 17a, with nozzle nomenclature in Figure 17b. Because of the pressure difference between the exit pressure (Pe), also known as back pressure, and the reservoir pressure, the flow through the nozzle reaches supersonic speeds [9].

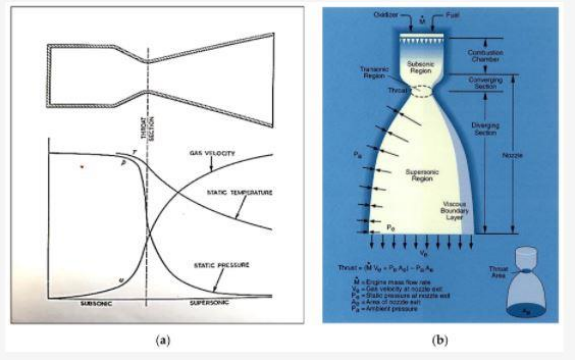

Figure 17: (a) Expansion in Convergent-Divergent Supersonic Nozzle and (b) Nozzle Geometrical Designations [9]

An imbalance between the throat static pressure and ambient pressure will result from the majority of the gross nozzle trust, which is generated by jet momentum with extra push from pressure. In contrast to convergent nozzles, the C-D nozzle permits expansion to occur inside the nozzle at high Nozzle Pressure Ratios (NPR = $^{p_t}/_{p_0}$) to maximize thrust output. The area ratio between the throat (A^*) and the exit region (A_e) has a major impact on the flow. The nozzle gradually expands in cross-sectional area downstream of the throat, forming the distinctive parabolic bell profile, which allows the exhausted gases to expand and generate the required thrust.

2.5.1. Nozzle Geometric Configurations

Conical Nozzle

Conical nozzles work by turning expelled gases into axial thrust, and they work best when the axial thrust is consistent across the nozzle axis [9]. As a result, smaller divergence angles (α) provide more axial thrust by maximizing the axial component of the exhaust exit velocity, resulting in a high specific impulse. However, this leads to longer and heavier nozzle diverging sections, which causes installation issues. Divergence losses occur when nozzles are shortened with large divergence angles. By the time the exhaust has passed the exit of a conical nozzle

with a semi-angle (α) divergent nozzle, the streamlines have diverged away from the axis of the jet, producing radial thrust instead.

Bell Nozzle

Bell-shaped nozzles are the most often used nozzle profile nowadays. In this scenario, nozzle profiling is customized to provide specific desirable pressure gradients in order to reduce flow separation and so improve the performance of the simple cone nozzle.

Two pieces make up bell-shaped nozzles. Near the throat, the nozzle outlines diverge at a wide angle before tapering off further downstream. The divergence angle near the nozzle exit is quite tiny, practically parallel to the jet axis. This arrangement maximizes performance while reducing weight, with the nozzle length being up to 25% less than the conical nozzle counterpart.

Dual Bell and Contoured Nozzle

The dual bell nozzle is a solution to the problems that traditional bell-shaped nozzles have with altitude expansion. In conventional nozzles, the contour inflection ensures a controlled and symmetrical separation, preventing the creation of high side loads of separated flow and enhancing thrust. The smaller nozzle's area ratio is significantly lower than that of the reference main engine nozzle, resulting in superior thrust performance at lower altitudes. Ascending to greater altitudes causes the separation point to depart the inflection point and migrate down the exit plane, where a higher area ratio of the nozzle extension delivers thrust with minimum altitude pressure losses.

There needs to be known area ratios between exit area and throat area, to determine the length of nozzle. Firstly, ratio of exit area to throat areas should be found. Related equation is shown below.

$$\frac{A}{A^*} = \frac{1}{M}\left(\frac{2}{\gamma+1}\left(1+\frac{\gamma-1}{2}M^2\right)\right)^{\frac{\gamma+1}{2(\gamma-1)}} \tag{9}$$

Nozzle Throat Area (A_8)	0,1138 m^2
Effective Throat Area (A_{8e})	0,11662 m^2
Exit Area(A_9)	0,5033 m^2
Area Ratio ($^{A}/_{A^*}$)	4,4233
Exit Velocity (u_9)	1711,5 $^{m}/_{s}$
Ideal Exit Velocity (u_{9i})	1729,56 $^{m}/_{s}$
Primary Nozzle Length (L_P)	0,1875 m
Secondary Nozzle Length (L_s)	0,5625 m
Primary Half Angle (θ)	14◦
Secondary Half Angle (α)	6◦

Table 2: Parameters of Nozzle

3. Result and Discussion

In this section, the desired parameters which are propulsive efficiency, thermal efficiency, overall efficiency, TSFC, specific impulse, and specific thrust are found depending on Mach number. To be able to get the most efficient values, MATLAB code (A.1) was prepared to obtain performance parameters. Mach numbers was iterated from 2 to 6 in order to get ramjet design Mach number. Our ramjet is operating in 15 km altitude. The detailed operation condition values are given in table below.

Altitude (m)	T_a (K◦)	P_a (Pa)
15000	232,75	12045

Table 1: Operating Conditions

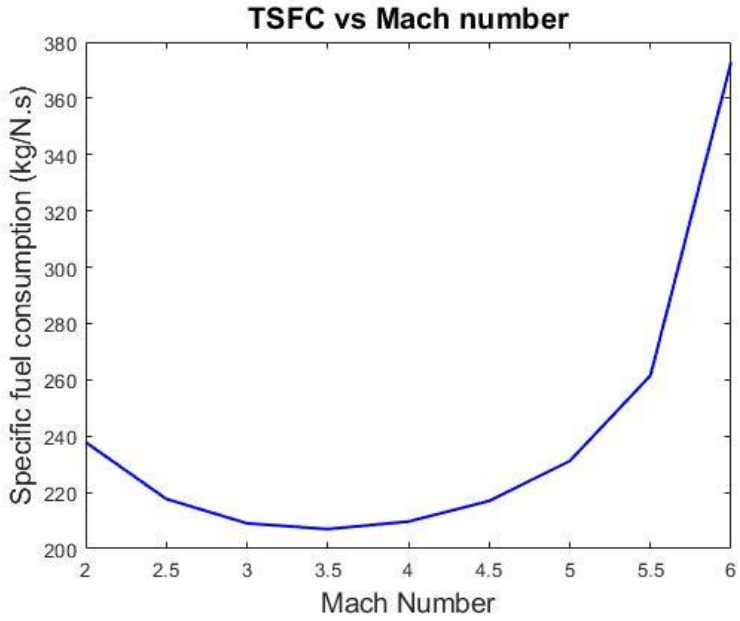

Figure 18: TSFC vs Mach Number

TSFC value need to be lowest value for an efficient ramjet engine because TSFC is the mass of fuel burned by an engine in one hour divided by the thrust. That means TSFC should be lowest for a fuel-efficient engine. Mach number initially was chosen with interrupting the lowest TSFC value because of deciding on the design Mach number. As it can be seen from Figure 18, TSFC is 206.952 kg/ (N. s) at 3.5 Mach and other Mach numbers have higher TSFC

values. Unlike TSFC, Specific impulse need to be highest value for efficient ramjet engine since the formula of specific impulse is inversely proportional compared to TSFC. Thus, specific impulse must be highest value at design Mach number. From Figure 19, specific impulse is equal to 1773.23 kg/ (N. s) at 3.5 Mach.

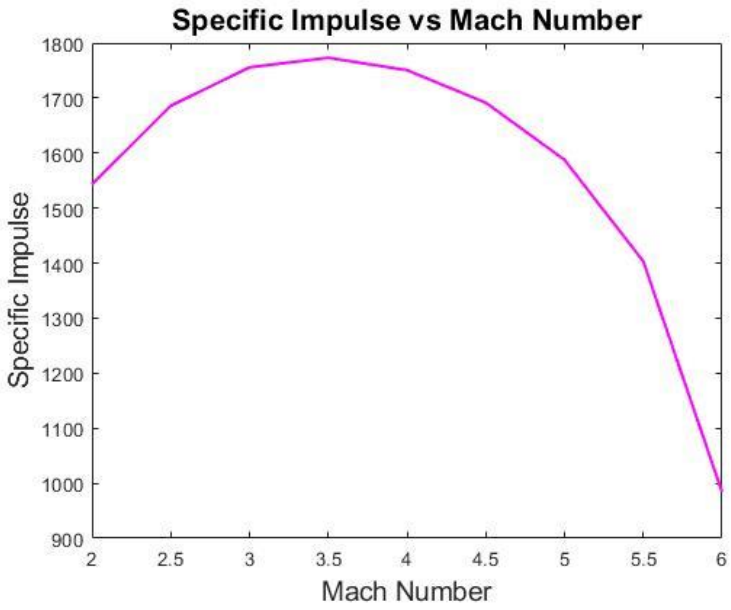

Figure 19: Specific Impulse vs Mach Number

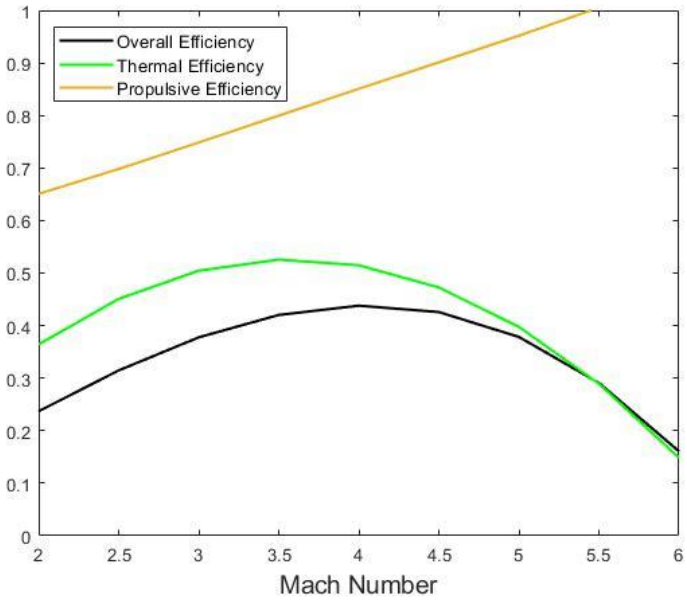

Figure 20: Overall, Thermal, and Propulsive Efficiencies vs Mach Number

Propulsion efficiency is the ratio of the available energy that is used for thrust to the energy which is supplied by the jet stream of the air. That means an efficient ramjet should deliver maximum thrust with low energy in terms of required thrust. Also, thermal efficiency represents the effectiveness with which the engine converts thermal energy into mechanical power. Thermal energy was chosen as Jet A which has heating value equals to 43.4 MJ/kg. In line with these parameters, thermal efficiency has highest value at design Mach number. Overall efficiency is the result of the multiplication of thermal efficiency and propulsive efficiency. In Figure 20, these three efficiencies are shown. Considering other desired parameters, the selected design Mach number is very efficient in these conditions.

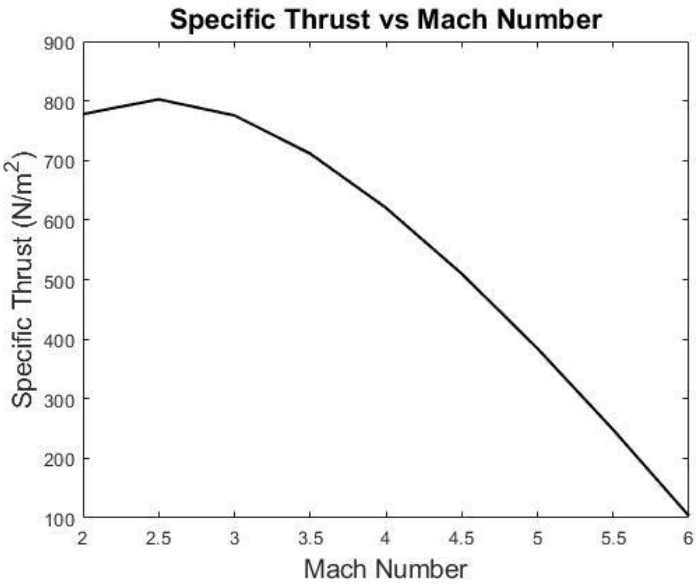

Figure 21: Specific Thrust vs Mach Number

Specific thrust is the thrust per unit air mass flowrate of a jet engine and can be calculated by the ratio of net thrust/total intake airflow. High-specific-thrust engines are often utilized at supersonic speeds, whereas extreme high-specific-thrust engines may reach hypersonic speeds. All parameters at 3.5 Mach are shown in Table 3.

	TSFC (kg/ (N. s))	Specific Impulse (kg/ (N. s))	Thermal Efficiency	Propulsive Efficiency	Overall Efficiency	Specific Thrust (N/m^2)
Value at 3.5 Mach Number	206.952	1773.23	0.5256	0.7997	0.4203	711.418

Table 3: Performance parameters at 3.5 Mach

After determining design Mach Number, MATLAB code (A.2) was written to obtain each ramp and shock wave angle. The velocity and pressure ratios for each ramp and shock angle are shown in the Table 4 and Table 5.

δ_1	ϑ_1	M_1	δ_2	ϑ_2	M_2	δ_3	ϑ_3	M_3	M_4
12.4286◦	26.6447◦	2,76	14.7143◦	33.9181◦	2,0896	17◦	46.0120◦	1,443	0,7223

Table 4: Intake Parameters

PR_1	PR_2	PR_3	PR_n	PRF
0.9063	0.9166	0.9286	0.9468	0.7304

Table 5: Pressure ratio each station and PRF

Since mixed-compression intake is used in this project, all oblique shocks are expected to occur external side of intake, whereas normal shock occur in throat which is internal part of the intake. Our design Mach number is selected as 3.5, therefore CFD results are obtained considering that Mach number.

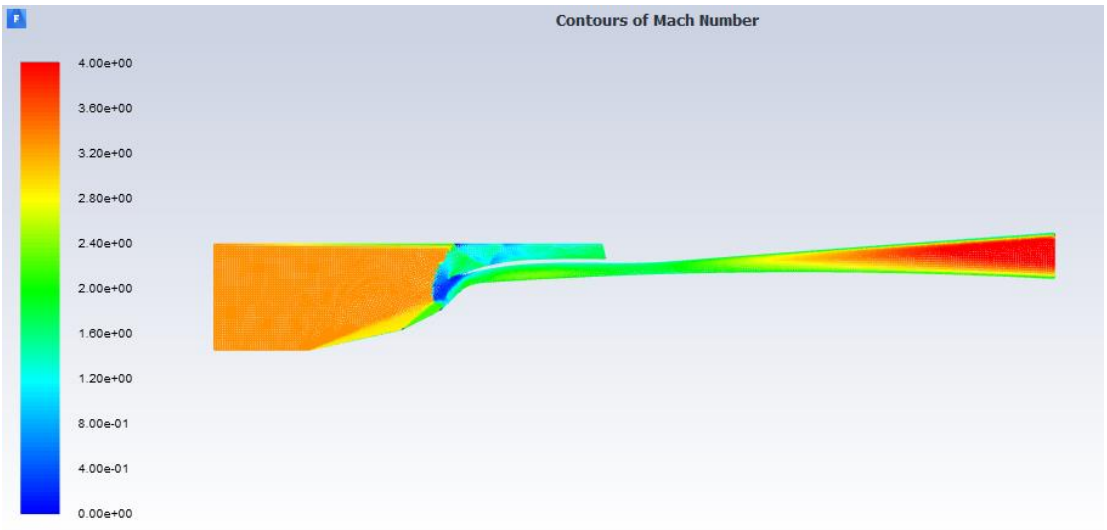

Figure 22 : Mach number contour plot

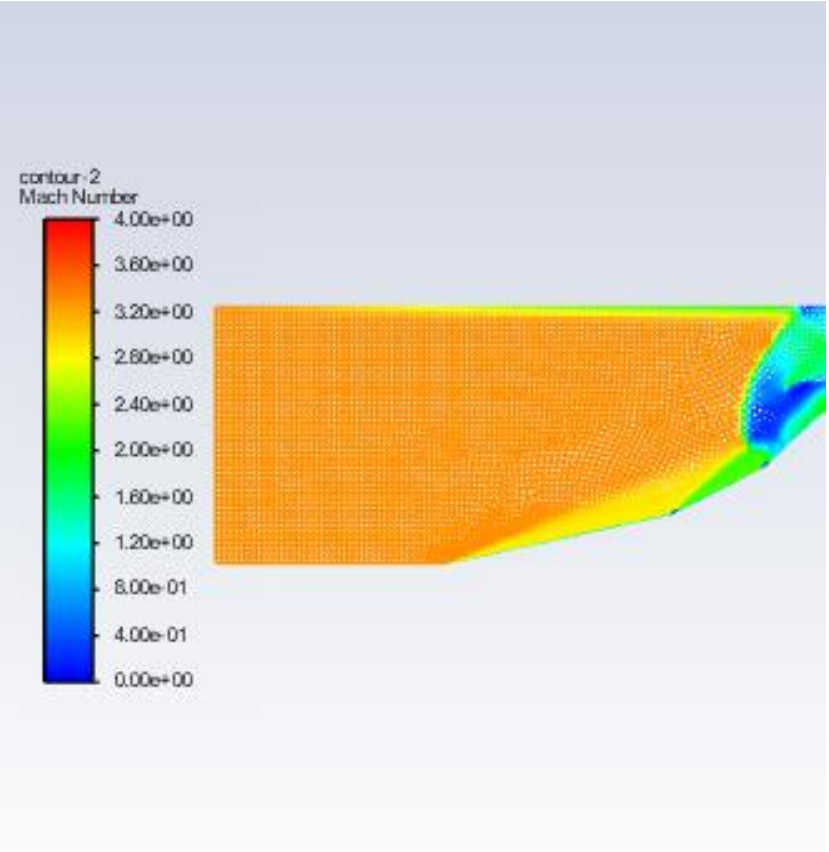

Figure 23 : Mach number contour plot

As it can be seen from the figures above, Mach numbers in each corresponding shock are matching with the values that we computed by using MATLAB Code (A.2). Mach number value is decreasing in each shock starting from design Mach number which is 3.5, and after three oblique shock and a normal shock value decrease to 0.7223.

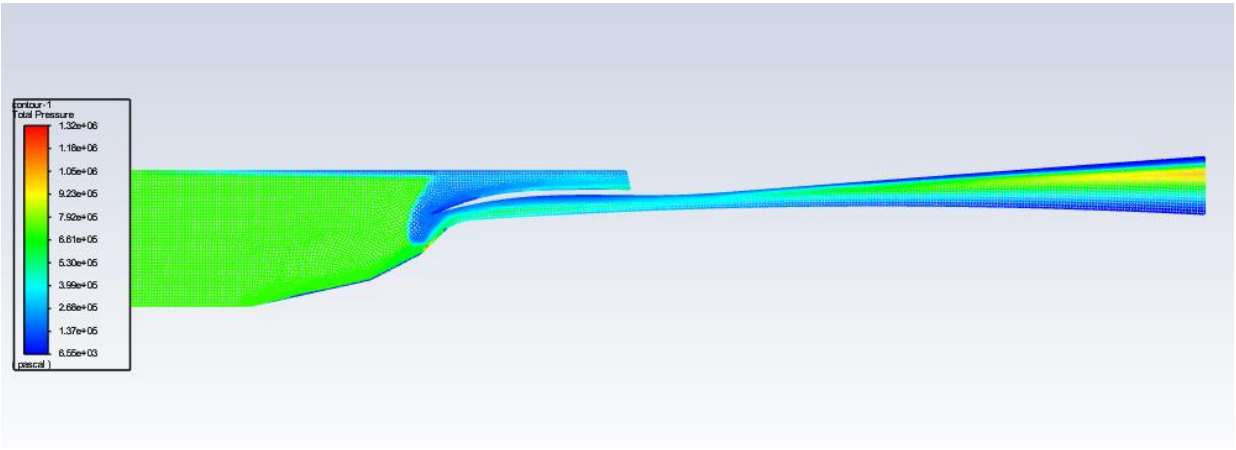

Figure 24 : Total pressure contour plot

Because any change in total pressure is considered as loss of performance, it is crucial to observe total pressure change throughout the intake. In Figure 25, total pressure decreases across each oblique shock and normal shock. Compared to oblique shock, total pressure decreases more across normal shock wave.

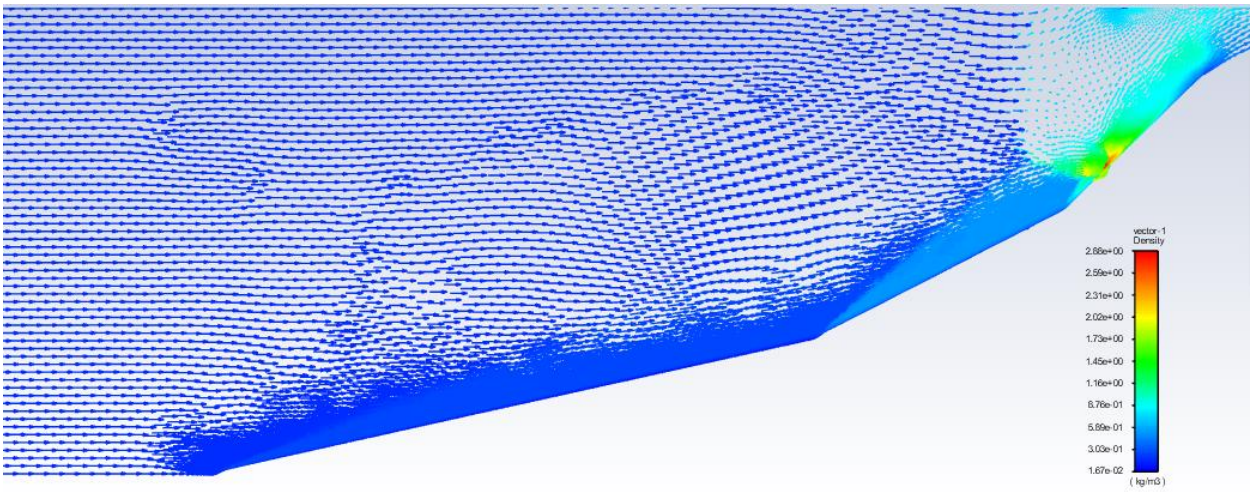

Figure 25: Density gradient vector plot

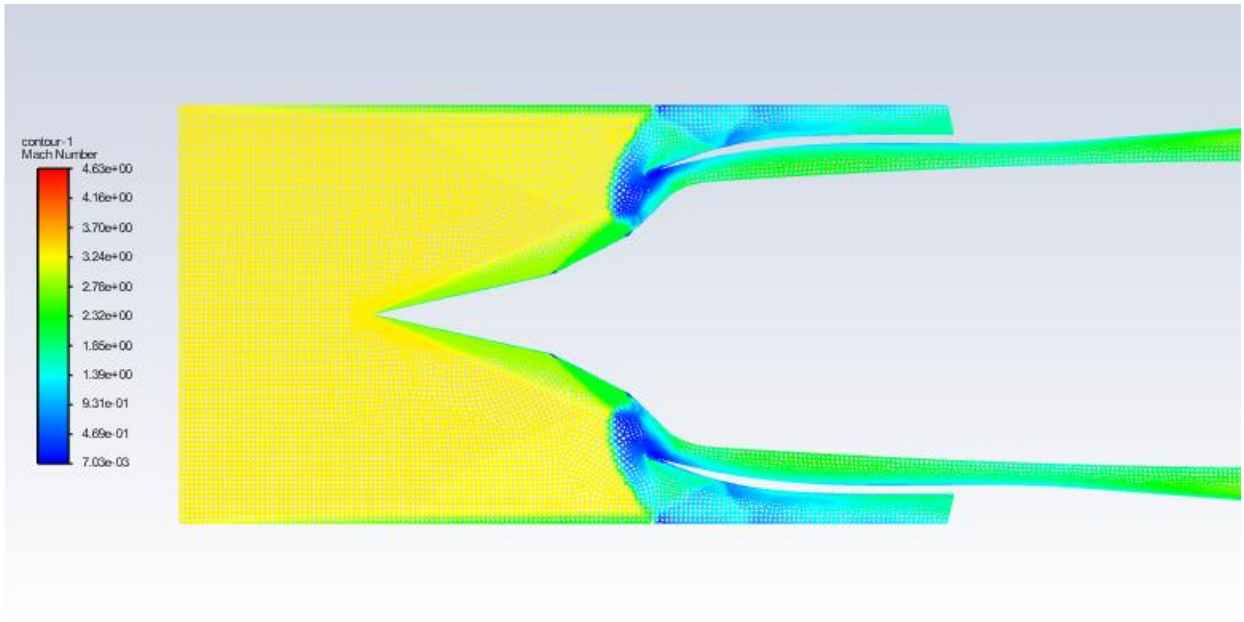

Figure 26: Full geometry of intake

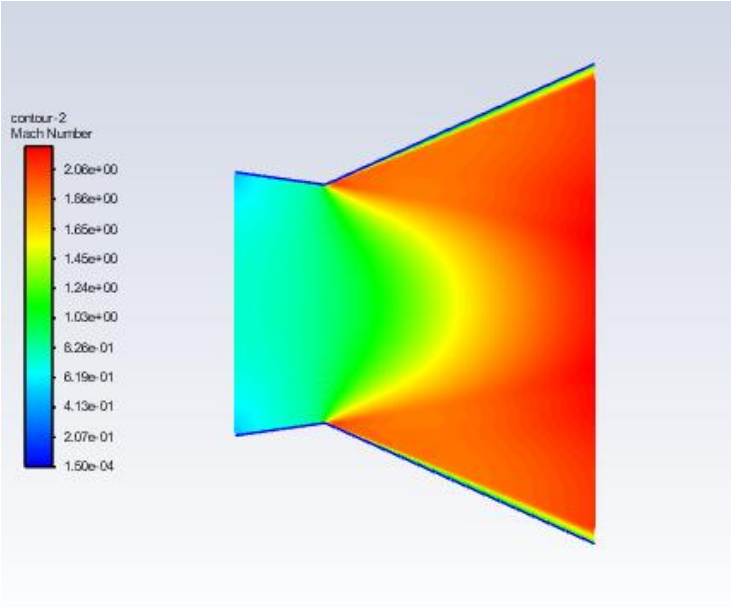

Figure 27 : Mach number contour of nozzle

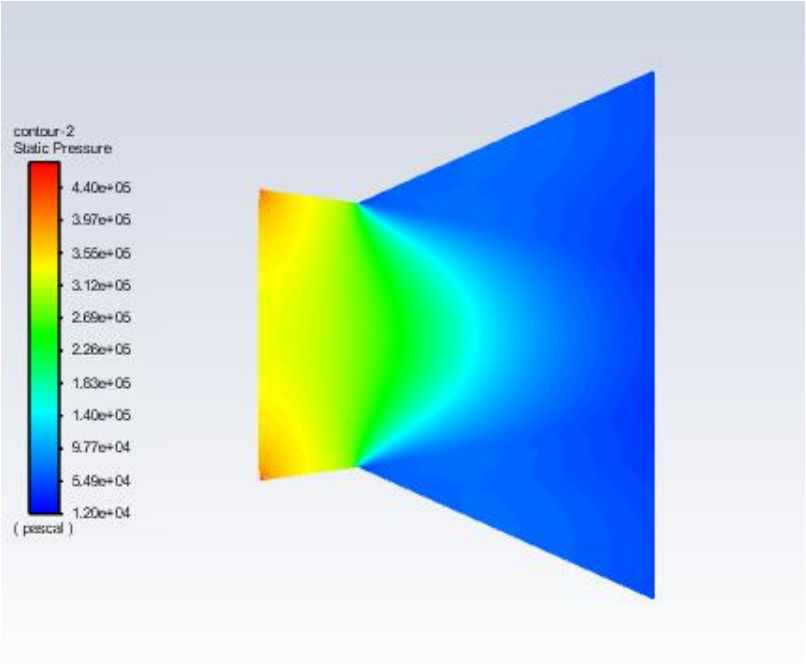

Figure 28: Static pressure contour of nozzle

It can be seen from figures above; Mach numbers are found in CFD simulation are almost same with our results which are obtained via MATLAB performance parameters code (A.1), and we

select our nozzle as perfectly expanded that is why the exit of nozzle is equal to atmospheric pressure which is 12045 Pa.

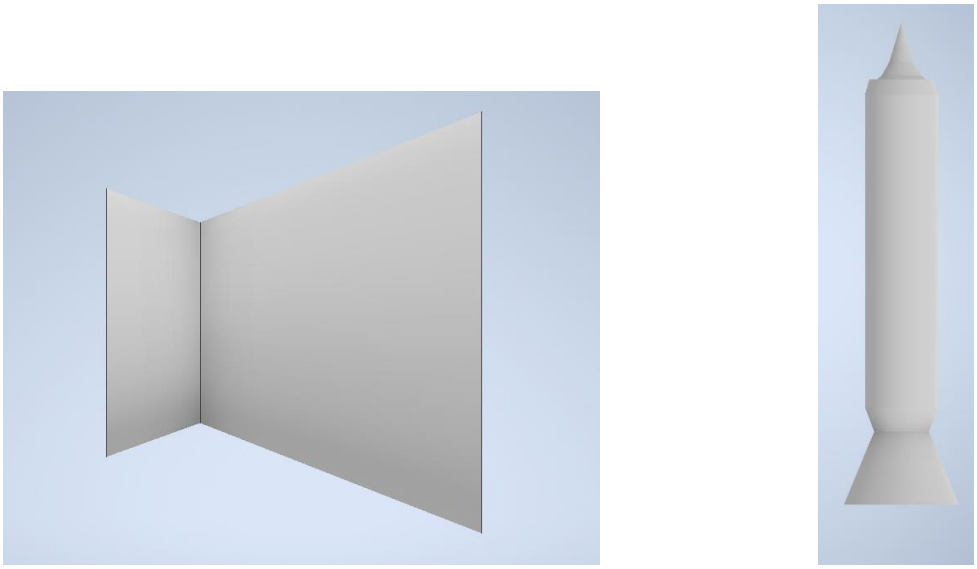

Figure 29: 3D view of Nozzle and Overall Ramjet

4. Conclusion

In conclusion, the goal of this project is developing a one-dimensional design tool using analytical and/or empirical, semi-empirical correlations to use for the conceptual and preliminary design of a ramjet engine to predict the performance of the engine at varying flight speeds, for Mach numbers ranging from 2 to 6. While there were focused on CFD analysis of engine intake and nozzle for the design point Mach number, also information about ramjet, applications, inlet types, combustion chamber and fuel injections of ramjets are also given. To design the most efficient engine, the optimum Mach number was found with TSFC. Looking at the other parameters in this Mach number, an efficient result was obtained in those parameters as well. At the same time, ramp angles and PRFs in the intake were found together with the design Mach number. The found PRF in intake is same as PRF according to MIL-E5008B (empirical correlations) standards used in its parameters. In order to confirm that results are found are correct or not, GasTurb is used as a benchmark. The GasTurb values are given in A.3. As in general, intake designs are done using design Mach number, so we implement same logic and then CFD results are coming up. With the help of ramp angle code, and performance parameters data, simulation is run, and important parameters are observed by using contour and vector plot's ability of ANSYS FLUENT.

5. References

[1] BOEING. (N.D.). IM-99A/B BOMARC MISSILE. Retrieved from https://www.boeing.com/history/products/im-99a-b-bomarc-missile.page

[2] Wood, M. Lockheed D-21 Air Launched Drone. Retrieved from http://www.wvi.com/~sr71webmaster/d21~1.htm

[3] Torp, V. (2016). Favourable Design of the Air Intake of a Ramjet.

[4] Sarah. (2018). Ramjet Part 3- Intake Geometry & Shock Waves. Retrieved from https://rocketgirl.blog/2018/05/12/ramjet-part-2-intake-geometry-shock-waves/

[5] Sabhadiya, Jignesh. (N.D.). What Is Combustion Chamber? - Function, And Types. Retrieved from https://www.engineeringchoice.com/combustion-chamber/

[6] Soares, Claire. (2008). Gas Turbines.

[7] Patel, A., Sahu, G., & Sen, P.K. (2015). International Journal of Engineering and Management Research. A Review on Fuel Injection System of Ramjet Engine.

[8] Farokhi, S. (2014). Aircraft propulsion. Chichester: J. Wiley

[9] Baidya et al. (2018). Ramjet Nozzle Analysis for Transport Aircraft Configuration for Sustained Hypersonic Flight. Retrieved from https://www.mdpi.com/2076-3417/8/4/574/htm

[10] Luu Hong Quan, Nguyen Phu Hung, Le Doan Quang, Vu Ngoc Long. Analysis and Design of a Scramjet Engine Inlet Operating from Mach 5 to Mach 10. International Journal of Mechanical Engineering and Applications. Vol. 4, No. 1, 2016, pp. 11-23. doi: 10.11648/j.ijmea.20160401.12

[11] Anderson, B., Peyster, D. A., Gad, S. C., Hakkinen, B. P. J., Kamrin, M., Locey, B., Mehendale, H. M., Pope, C., Shugart, L., & Wexler, P. (2005). Encyclopedia of Toxicology, Four-Volume Set: ENCYCLOPEDIA OF TOXICOLOGY, Second Edition (2nd ed.). Academic Press.

[12] Sforza, P. M. (2017). AEROSPACE PROPULSION FUELS. In Theory of aerospace propulsion. Elsevier, Second Edition

[13] ASE 435 Lecture Notes

6. Appendix

MATLAB Code (A.1)

```
clear all
close all
clc

TSFC = zeros;
I_s = zeros;
n_propulsive = zeros;
n_thermal = zeros;
n_overall = zeros;
Specific_Thrust = zeros;


%%variables

i = 1 ;
M_i = [2 2.5 3 3.5 4 4.5 5 5.5 6];
T_a = 232.75;
P_a = 12045;
gama = 1.4;
c_p =1004;
Tt4 = 2300;
g_0 = 9.81;
Q_r = 43400000;
R =  (c_p * (gama - 1))/gama;
rho_a = P_a /(T_a * R);
a_a = sqrt(gama*T_a*R);



%%efficiencies are defined

dif_eff = 0.9;
burner_eff = 0.9;
pres_ratio_burner = 0.9;
nozzle_eff = 0.95;
pres_ratio_nozzle= 1;
Tt9 = 2245;
A_1 = 0.307;




while i < 10

%% Station Calculations


u_a = a_a * M_i(i) ;
m_dot= A_1*(rho_a * u_a)
Tt0(i) = T_a * ( 1 + ((gama-1)/2)*M_i(i)^2);
Tt2(i) = Tt0(i);
Pt0(i) = P_a * (1 + dif_eff*((gama-1)/2)*M_i(i)^2)^(gama/(gama-1));

if M_i(i) < 5
```

```
PRF = 1 - 0.075 * (M_i(i) - 1)^1.35;
else
PRF = 800/(M_i(i)^4 + 935);
end

Pt2(i) = Pt0(i) * PRF;



Pt4= Pt2(i) * pres_ratio_burner;

P9(i) = P_a;

f(i) = (Tt4 - Tt0(i))/(Q_r * burner_eff/(c_p) - Tt4);
mf(i) = f(i) * m_dot ;
Pt9 = Pt4 * pres_ratio_nozzle;
M_9(i) = sqrt((2/(gama-1)) * (((Pt9 / P9(i))^((gama-1)/gama)) - 1))
T9 = Tt9 / (1 + ((gama-1)/2)*M_9(i)^2) ;
a_9 = sqrt(gama*R*T9);
u_9(i) = a_9 * M_9(i) ;
Thrust(i) = ((m_dot + mf(i)) *u_9(i) -m_dot* u_a) + 0.919*(P9(i)-P_a);



%% Performance Parameters

TSFC_1(i) = mf(i) / Thrust(i) ;
TSFC(i) = (TSFC_1(i) * 3600 / 10^-3);
I_s(i) = 1 / (g_0 * TSFC_1(i));
n_propulsive(i) = 2*(Thrust(i)*u_a)/((m_dot+mf(i))*(u_9(i))^2-m_dot*(u_a)^2);
n_thermal(i) = ((1 + f)*u_9(i)^2 - u_a^2)/(2*f*Q_r*burner_eff);
n_overall(i) = n_propulsive(i) * n_thermal(i) ;
Specific_Thrust(i) = Thrust(i) / m_dot ;



%% iteration initializer
i = i+1;

end

%%plots

figure(1)
plot(M_i,TSFC,'blue','LineWidth', 1.5)
title('TSFC vs Mach number','FontSize',15)
xlim([2 6]);
xlabel('Mach Number','FontSize',14)
ylabel('Specific fuel consumption (kg/N.s)','FontSize',14)
hold on

figure(2)
plot(M_i,I_s,'Magenta','LineWidth', 1.5)
title('Specific Impulse vs Mach Number','FontSize',15)
xlim([2 6]);
xlabel('Mach Number','FontSize',14)
ylabel('Specific Impulse','FontSize',14)
hold on
```

```
figure(3)
plot(M_i,n_propulsive,'LineWidth', 1.5)
title('Propulsive Efficiency vs Mach Number','FontSize',15)
xlim([2 6]);
ylim([0.5 1]);
xlabel('Mach Number','FontSize',14)
ylabel('Propulsive Efficiency','FontSize',14)
hold on

figure(4)
plot(M_i,n_thermal,'green','LineWidth', 1.5)
title('Thermal Efficiency vs Mach Number','FontSize',15)
xlim([2 6]);
ylim([0 0.8]);
xlabel('Mach Number','FontSize',14)
ylabel('Thermal Efficiency','FontSize',14)
hold on

figure(5)
plot(M_i,Specific_Thrust,'black','LineWidth', 1.5)
title('Specific Thrust vs Mach Number','FontSize',15)
xlim([2 6]);
xlabel('Mach Number','FontSize',14)
ylabel('Specific Thrust (N/m^2)','FontSize',14)
hold on

figure(6)
plot(M_i,n_overall,'black', 'LineWidth', 1.5);
title('Overall Efficiency vs Mach Number ','FontSize',15)
xlim([2 6]);
ylim([0 0.6]);
xlabel('Mach Number','FontSize',14)
ylabel('Overall Efficiency','FontSize',14)
hold on

figure(7)
plot(M_i,n_overall,'black', 'LineWidth', 1.5);
hold on
plot(M_i,n_thermal,'green','LineWidth', 1.5)
hold on
plot(M_i,n_propulsive,'LineWidth', 1.5)
legend('Overall Efficiency','Thermal Efficiency','Propulsive
Efficiency','FontSize',12);
xlim([2 6]);
ylim([0 1]);
xlabel('Mach Number','FontSize',14)
hold on
```

MATLAB Code (A.2)

```
clc
clear all
close all
% Design Parameters %
Minf = 3.5;
syms p0;
gamma = 1.4;
N = 17;
```

```
N1 = 30;
% The Flow Deflection Angle ( Up to 8 Degree) %
theta1(:,1,1) = linspace(1,N,N1)/180*pi;
theta2(1,:,1) = linspace(1,N,N1)/180*pi;
theta3(1,1,:) = linspace(1,N,N1)/180*pi;
% Local Static Pressure %
pinf = p0*((1 + (gamma - 1)/2*(Minf^2))^(-gamma/(gamma - 1)));
% Freestream to Region 1 - Oblique Shock
for i = 1:N1
 beta1(i,1,1) =fzero(@(beta) 2.*cot(beta).*((Minf.^2).*(sin(beta).^2)-
1)./((Minf.^2).*(gamma+cos(2.*beta))+2)-tan(theta1(i,1,1)),[theta1(i,1,1),1]);
 Mn_inf(i,1,1) = Minf*sin(beta1(i,1,1));
 Mn1(i,1,1) = sqrt((1 + (gamma-1)/2*(Mn_inf(i,1,1)^2))/(gamma*(Mn_inf(i,1,1)^2) -
(gamma - 1)/2));
 M1(i,1,1) = Mn1(i,1,1)/sin(beta1(i,1,1) -theta1(i,1,1));
 p1(i,1,1) = pinf*(1 + (2*gamma)/(gamma + 1)*((Mn_inf(i,1,1)^2) - 1));
 p_01(i,1,1) = p1(i,1,1)*((1 + (gamma - 1)/2*(M1(i,1,1)^2))^(gamma/(gamma -1)));
end
% Region 1 to Region 2 - Oblique Shock
for i = 1:N1
 for j = 1:N1
 beta2(i,j,1) =fzero(@(beta) 2.*cot(beta).*((M1(i,1,1).^2).*(sin(beta).^2)-
1)./((M1(i,1,1).^2).*(gamma+cos(2.*beta))+2)-
tan(theta2(1,j,1)),[theta2(1,j,1),1]);
 Mn1(i,j,1)= M1(i,1,1)*sin(beta2(i,j,1));
 Mn2(i,j,1)= sqrt((1 + (gamma -1)/2*(Mn1(i,j,1)^2))/(gamma*(Mn1(i,j,1)^2) - (gamma
-1)/2));
 M2(i,j,1) = Mn2(i,j,1)/sin(beta2(i,j,1) - theta2(1,j,1));
 p2(i,j,1) = p1(i,1,1)*(1 + (2*gamma)/(gamma + 1)*((Mn1(i,j,1)^2) - 1));

 p_02(i,j,1)= p2(i,j,1)*((1 + (gamma - 1)/2*(M2(i,j,1)^2))^(gamma/(gamma -1)));
 end
end
% Region 2 to Region 3 - Oblique Shock
for i = 1:N1
 for j = 1:N1
 for k=1:N1
 beta3(i,j,k) =fzero(@(beta) 2.*cot(beta).*((M2(i,j,1).^2).*(sin(beta).^2)-
1)./((M2(i,j,1).^2).*(gamma+cos(2.*beta))+2)-
tan(theta3(1,1,k)),[theta3(1,1,k),1]);
 Mn2(i,j,k)= M2(i,j,1)*sin(beta3(i,j,k));
 Mn3(i,j,k)= sqrt((1 + (gamma -1)/2*(Mn2(i,j,k)^2))/(gamma*(Mn2(i,j,k)^2) - (gamma
-1)/2));
 M3(i,j,k) = Mn3(i,j,k)/sin(beta3(i,j,k) - theta3(1,1,k));
 p3(i,j,k) = p2(i,j,1)*(1 + (2*gamma)/(gamma + 1)*((Mn2(i,j,k)^2) - 1));
 p_03(i,j,k)= p3(i,j,k)*((1 + (gamma - 1)/2*(M3(i,j,k)^2))^(gamma/(gamma -1)));

 end
 end
end
%Normal Shock
for i = 1:N1
 for j = 1:N1
 for k=1:N1
 M4(i,j,k) = sqrt((1 + (gamma - 1)/2*(M3(i,j,k)^2))/(gamma*(M3(i,j,k)^2) - (gamma
- 1)/2));
 p4(i,j,k) = p3(i,j,k)*(1 + (2*gamma)/(gamma + 1)*((M3(i,j,k)^2) - 1));
 p04(i,j,k) = p4(i,j,k)*((1 + (gamma - 1)/2*(M4(i,j,k)^2))^(gamma/(gamma - 1)));
 end
```

```
 end
end
% Performance Parameters
PRF = p04/p0;
PRF = double(PRF);
MaxPRF = max(PRF,[],'all')
[row, col, dim3] = ind2sub(size(PRF), find(PRF == max(PRF(:))))
FirstDefAngle=theta1(row)*180/pi
FirstShockWaveAngle=beta1(row)*180/pi
FirstMach=M1(row)
SecondDefAngle=theta2(col)*180/pi

SecondShockWaveAngle=beta2(row,col)*180/pi
SecondMach=M2(row,col)
ThirdDefAngle=theta3(dim3)*180/pi
ThirdShockWaveAngle=beta3(row,col,dim3)*180/pi
ThirdMach=M3(row,col,dim3)
FourthMach=M4(row,col,dim3)
prate1=p_01(row)/p0;
prate1=double(prate1)
prate2=p_02(row,col)/p0;
prate2=double(prate2)
prate3=p_03(row,col,dim3)/p0;
prate3=double(prate3)
```

A.3

GasTurb Data

Station	W kg/s	T K	P kPa	WRstd kg/s			
amb		188,65	12,045		FN	=	42,21 kN
1		643,46	927,847		TSFC	=	95,4332 g/(kN*s)
2	68,167	643,46	688,098	15,000	WF	=	4,02866 kg/s
61	65,440	643,46	619,288		FN/W2	=	619,28 m/s
7	69,469	2300,00	588,061		P2/P1	=	0,7416
8	72,196	2241,08	588,061		A8	=	0,1493 m²
					P8/Pamb	=	48,8238
Burner Efficiency			0,9000		A61	=	0,26203 m²
Jetpipe Diam.			0,5776		XM61	=	0,15000
Pressure Loss [%]			5,04		XM7	=	0,35060

hum [%]	war0	FHV	Fuel
0,0	0,00000	43,400	Generic

	Units	St 2	St 6	St 61	St 7	St 8
Mass Flow	kg/s	68,167	68,167	65,4403	69,469	72,1957
Total Temperature	K	643,457	643,457	643,457	2300	2241,08
Static Temperature	K	614,934	638,726	638,726	2230,93	1985,91
Total Pressure	kPa	688,098	619,288	619,288	588,061	588,061
Static Pressure	kPa	581,781	602,6	602,6	505,539	325,292
Velocity	m/s	246,239	100,284	100,284	443,207	847,122
Area	m²	0,083993	0,206818	0,198545	0,198545	0,149346
Mach Number		0,5	0,2	0,2	0,49478	1
Density	kg/m³	3,29589	3,28667	3,28667	0,789451	0,570653
Spec Heat @ T	J/(kg*K)	1061,39	1061,39	1061,39	1425,42	1415,15
Spec Heat @ Ts	J/(kg*K)	1054,57	1060,26	1060,26	1420,77	1395,93
Enthalpy @ T	J/kg	354983	354983	354983	2,57322E6	2,48014E6
Enthalpy @ Ts	J/kg	324666	349955	349955	2,475E6	2,12133E6
Entropy Function @ T		2,7445	2,7445	2,7445	8,67359	8,51623
Entropy Function @ Ts		2,57666	2,71718	2,71718	8,52239	7,92412
Exergy	J/kg	448649	442944	442944	2,33746E6	2,25289E6
Gas Constant	J/(kg*K)	287,05	287,05	287,05	287,04	287,04
Fuel-Air-Ratio		0	0	0	0,061562	0,0591
Water-Air-Ratio		0	0	0	0	0